

# Nanothallium(III) sulfide from dithiocarbamate precursors: Synthesis, single crystal X-ray structures and characterization



G.S. Sivagurunathan<sup>a</sup>, K. Ramalingam<sup>a,\*</sup>, C. Rizzoli<sup>b</sup>

<sup>a</sup>Department of Chemistry, Annamalai University, Annamalaiagar 608 002, Tamil Nadu, India

<sup>b</sup>Department of General and Inorganic Chemistry, University of Parma, Parma 43100, Italy

## ARTICLE INFO

### Article history:

Received 29 March 2013

Accepted 4 August 2013

Available online 14 August 2013

### Keywords:

Nanothallium sulfide

Dithiocarbamate

EDX

TEM

X-ray crystal structures

## ABSTRACT

Nanothallium sulfide was formed from  $Tl(chmdtc)_3$  (**1**),  $Tl(chedtc)_3$  (**2**) and  $Tl(dchdct)_3$  (**3**) (where  $chmdtc$  = cyclohexyl methyl dithiocarbamate,  $chedtc$  = cyclohexylethyl dithiocarbamate,  $dchdct$  = dicyclohexyl dithiocarbamate). Single crystal structures of the complexes are reported. The ease of formation was the highest for (**3**) and is in line with the longest mean Tl–S and thioureide C–N bonds observed for (**3**). The *nano* metal sulfide formed is spherical in nature and has been characterized by PXRD, EDX, TEM.  $Tl_4S_3$  was stable up to 300 °C. Thioureide stretching bands are observed at 1471, 1468, 1448  $cm^{-1}$  for (**1**), (**2**) and (**3**) respectively. Thioureide stretching band of (**3**) is significantly lower than others due to steric effect of cyclohexyl substituents. Thallium(III) complexes exhibit fully allowed charge transfer transitions (CT) which appeared as intense absorptions.  $^1H$  NMR shows that the  $\alpha$ -CH and  $\alpha'$ -CH<sub>3</sub> protons are affected to a maximum effect on complexation.  $^{13}C$  NMR spectra show thioureide carbon signal around 200 ppm.

© 2013 Elsevier Ltd. All rights reserved.

## 1. Introduction

Coordination chemistry of thallium(III) shows rich geometry and chemical properties in its compounds. Thallium and its compounds find extensive application in many fields. Various thallium compounds have been used as chemical tracers in diagnosis, particularly in cardiology [1,2]. Thallium is an important ingredient in high temperature oxide superconductors [3,4]. Thallium compounds are useful in the production of optical glass, lenses for IR equipment and scintillation sensors [5]. Thallium mono sulfide is an incongruent compound and it is used as a semiconductor [6,7]. Thallium chalcogenide coated polymers find use in photonic applications [8,9]. Thallium reacts with nitrogen donors to form stable coordination compounds [10]. Dithiocarbamates are highly versatile ligands towards main group metals and recently we established that the metal dithiocarbamates are useful precursors to produce respective metal sulfides as nano materials [11–13]. In our continued interest in the production of nano thallium sulfides from the corresponding thallium dithiocarbamates, structural and chemical investigations have been carried out [14,15]. In this paper we report the synthesis, spectroscopic, electrochemical analysis and single crystal X-ray structures of  $[Tl(chmdtc)_3]$  (**1**),  $[Tl(chedtc)_3]$  (**2**),  $[Tl(dchdct)_3]$  (where  $chmdtc$  = cyclohexylmethyl dithiocarbamate,  $chedtc$  = cyclohexylethyl dithiocar-

bamate,  $dchdct$  = dicyclohexyldithiocarbamate anions) (**3**). Nanothallium(III) sulfide was prepared by non conventional solvothermal decomposition of (**1**) and was characterized by powder XRD, EDX and HRTEM analysis.

## 2. Experimental

All the reagents and solvents employed were commercially available analytical grade materials and were used as supplied, without further purification. IR spectra were recorded as KBr pellets on ABB Bomem MB 104 spectrometer (range 4000–400  $cm^{-1}$ ). Electronic spectra were recorded in dichloromethane on a HITACHI U-2001 spectrometer. Cyclic voltammetric studies were carried out using a CH1604C electrochemical analyzer. NMR spectra were recorded on a Bruker 400 MHz spectrometer at room temperature using  $CDCl_3$  as solvent. The diffraction intensities of the poly crystalline  $Tl_4S_3$  samples were collected in the  $2\theta$  range 2–80° using Bruker-D8 powder X-ray diffractometer equipped with  $Cu K\alpha$  radiation at fixed current and potential. The scan speed and step size were 0.05  $min^{-1}$  and 0.00657 respectively. SEM and EDS analysis on the samples were carried out with JEOL JSM – 5610 LV instrument.

### 2.1. X-ray crystallography

Intensity data were collected at ambient temperature (295 K) on Bruker SMART 1000 CCD diffractometer using graphite

\* Corresponding author. Tel.: +91 413 2202834; fax: +91 414 42265.

E-mail address: [krauchem@yahoo.com](mailto:krauchem@yahoo.com) (K. Ramalingam).

monochromated Mo K $\alpha$  radiation ( $\lambda = 0.71073 \text{ \AA}$ ). Data were corrected for absorption using the SADABS program and  $\omega$ -scan technique was used for data collection [16,17]. The structures were solved by SIR97 [18] and were refined by full matrix least squares with SHELXL-97 [19]. All the non-hydrogen atoms were refined anisotropically and the hydrogen atoms were fixed geometrically. ORTEP-3 program was used for drawing the molecular plots [20].

## 2.2. Synthesis of the complexes and non conventional solvothermal preparation of thallium sulfide

### 2.2.1. Preparation of thallium(III) chloride

Thallium(III) chloride was prepared by the oxidation of thallium(I) chloride with chlorine [14]. Thallium(I) chloride (0.24 g, 1 mmol) was added with 15 mL of acetonitrile under stirring. Chlorine gas was passed through the suspension with continuous stirring, thallium(III) chloride being completely soluble in acetonitrile a clear solution was formed after some time. After the formation of thallium(III) chloride, nitrogen gas was passed through the acetonitrile solution in order to remove excess chlorine gas. Thallium(III) chloride in solid state decomposes at  $\sim 40^\circ\text{C}$  and hence the acetonitrile solution was used as such in the preparation of the complexes. Yield of thallium(III) chloride as acetonitrile solution was found to be 82%.

### 2.2.2. Synthesis of tris(cyclohexylmethyldithiocarbamato)thallium(III)(1)

Cyclohexylmethyl amine (0.4 mL, 3 mmol) in acetonitrile (25 mL) and carbon disulfide (0.24 mL, 3 mmol) in acetonitrile were mixed under ice cold condition ( $5^\circ\text{C}$ ) to obtain yellow dithiocarbamic acid solution. To the freshly prepared dithiocarbamic acid solution acetonitrile solution of  $\text{TlCl}_3$  (0.34 g, 1 mmol) was added drop by drop with constant stirring for about an hour. An orange yellow solid separated from the mixture which was filtered, washed with acetonitrile and dried in air. The separated compound was recrystallized from toluene. Yield: 78%; mp:  $196^\circ\text{C}$ .

### 2.2.3. Synthesis of tris(cyclohexylethyldithiocarbamato)thallium(III)(2)

Cyclohexylethylamine (0.45 mL, 3 mmol) in acetonitrile 25 mL, carbon disulfide (0.24 mL, 3 mmol) and  $\text{TlCl}_3$  (0.34 g, 1 mmol) were used and the procedure as described in 2.3.2 was followed. Yield: 68%; mp:  $180^\circ\text{C}$ .

### 2.2.4. Synthesis of tris(dicyclohexyldithiocarbamato)thallium(III)(3)

Dicyclohexylamine (0.59 mL, 3 mmol) in acetonitrile 25 mL, carbon disulfide (0.24 mL, 3 mmol) and  $\text{TlCl}_3$  (0.34 g, 1 mmol) were used and a procedure as described in 2.3.2 was followed. Yield: 70%; mp:  $242^\circ\text{C}$ .

### 2.2.5. Preparation of $\text{Tl}_4\text{S}_3$ by nonconventional solvothermal decomposition of $[\text{Tl}(\text{chmdtc})_3]$

A mixture of tris(cyclohexylmethyldithiocarbamato) thallium(III) (0.7 g) as a clear solution in chloroform (100 mL) was heated with diethylenetriamine (2 mL) at  $60^\circ\text{C}$  for 45 min. Black  $\text{Tl}_4\text{S}_3$  obtained was decanted from chloroform, washed with ether, chloroform in a drop of dodecylamine and was dried in air. Yield: 71%. Similar procedure was adopted for the preparation of  $\text{Tl}_4\text{S}_3$  from compounds (2) and (3). Yields of  $\text{Tl}_4\text{S}_3$  from (2) and (3) are 69% and 75% respectively. The ease of formation of thallium sulfide was found to be very high for (3) compared to the other two compounds.

## 3. Results and discussion

### 3.1. Characterization of thallium sulfide

#### 3.1.1. Powder XRD analysis

Fig. 1 shows the powder XRD patterns of  $\text{Tl}_4\text{S}_3$ . The prepared compound shows two prominent signals (Fig. 1A) at  $2\theta = 32.83^\circ$  and  $23.05^\circ$  which agreed well with the JCPDS No. 43-1067 for  $\text{Tl}_4\text{S}_3$ . An earlier report on thin films of  $\text{Tl}_4\text{S}_3$  indicated that the heating of the film at  $300^\circ\text{C}$  converted it to  $\text{Tl}_2\text{S}$  completely [6]. The converted thin film,  $\text{Tl}_2\text{S}$  showed an intense signal at  $2\theta = 29.45^\circ$ , in agreement with the JCPDS No. 29-1344 and the two prominent signals at  $2\theta = 32.83^\circ$  (220) and  $23.05^\circ$  ( $-211$ ) characteristic of  $\text{Tl}_4\text{S}_3$  totally vanished on heating at  $300^\circ\text{C}$ . In this study, on heating  $\text{Tl}_4\text{S}_3$  to  $300^\circ\text{C}$  the PXRD pattern showed increase in intensity of  $32.83^\circ$  and  $23.05^\circ$  signals compared to that at room temperature as shown in Fig. 1. The signal corresponding to  $\text{Tl}_2\text{S}$  at  $2\theta = 29.45^\circ$  did not appear at  $300^\circ\text{C}$ . Therefore, the present investigation reveals that the bulk  $\text{Tl}_4\text{S}_3$  is stable up to  $300^\circ\text{C}$  and does not transform to  $\text{Tl}_2\text{S}$ .

#### 3.1.2. EDX, HRTEM analysis

EDX of  $\text{Tl}_4\text{S}_3$  is shown in Fig. 2. The metal sulfide obtained shows spherical nature of the particles and EDX confirmed the presence of thallium and sulfur. HRTEM and SAED of the sample are shown in Fig. 3. The spherical nature of the particles is confirmed by the TEM micrographs and the particles are in the range of 20 nm.

### 3.2. Characterization of the dithiocarbamate precursors

#### 3.2.1. Infrared spectral studies

Table 1 lists important spectral and cyclicvoltammetric data. In the IR spectra of the compounds, the characteristic thioureide stretching bands are observed at  $1471 \text{ cm}^{-1}$  for  $\text{Tl}(\text{chmdtc})_3$  (1)  $1468 \text{ cm}^{-1}$  for  $\text{Tl}(\text{chedtc})_3$  (2) and  $1448 \text{ cm}^{-1}$  for  $\text{Tl}(\text{dchdct})_3$  (3) respectively. The stretching band of (3) is significantly lower than those observed in (1) and (2) due to the steric effect of two bulky

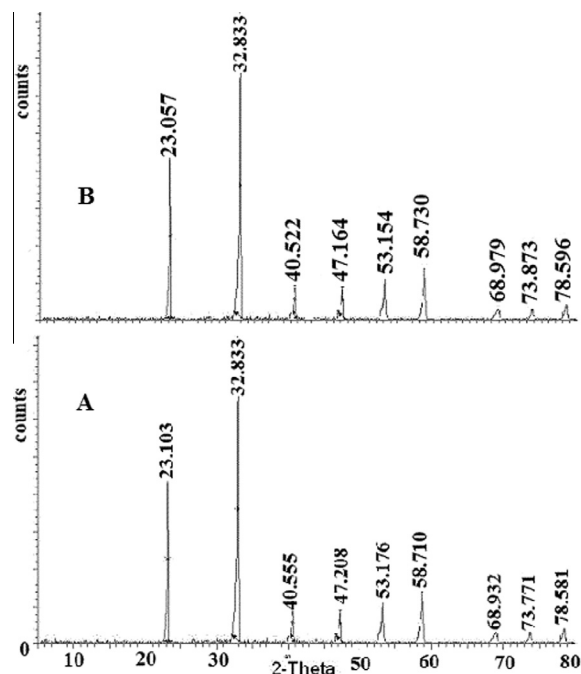
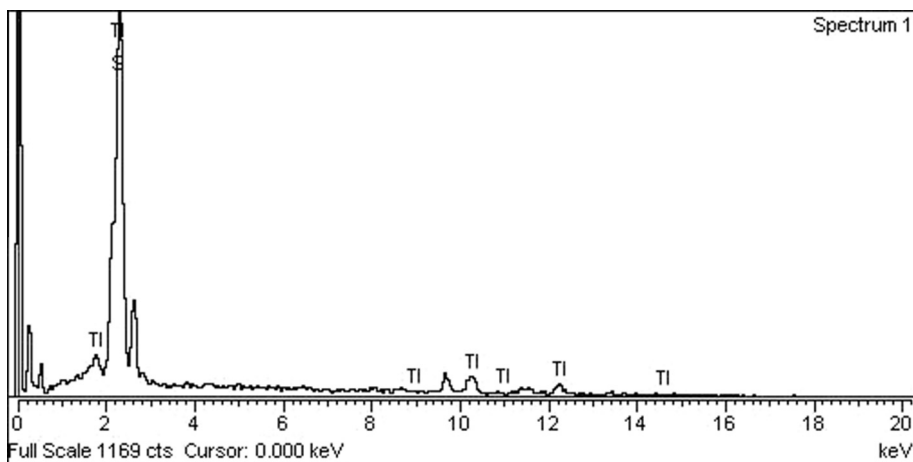
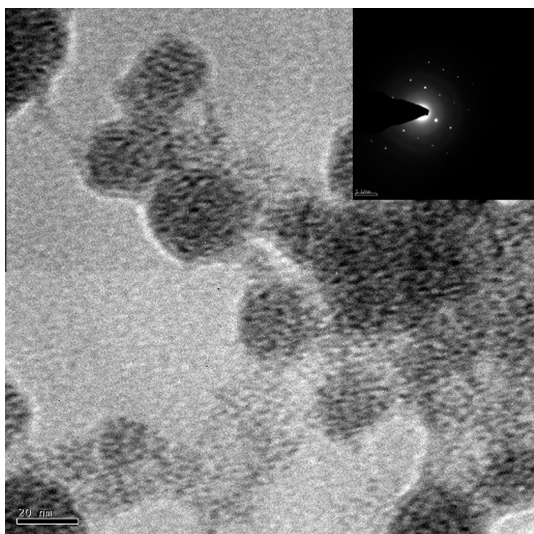


Fig. 1. Powder XRD patterns of  $\text{Tl}_4\text{S}_3$ , (A) at room temperature, (B) at  $300^\circ\text{C}$ .

Fig. 2. EDX of  $Tl_4S_3$ .Fig. 3. HRTEM and SAED of  $Tl_4S_3$ .

**Table 1**  
Electronic, IR and cyclic voltammetric parameters.

Compound	UV-Vis (nm)		IR ( $cm^{-1}$ )			CV (mV)		
	CT	$\pi-\pi^*$	$\nu_{C-N}$	$\nu_{C-S}$	$\nu_{C-H}$	Cathodic	Anodic	
(1)	324	259	1471	1006	2853	-972	-1500	-767
(2)	326	260	1468	1017	2853	-1117	-1566	-890
(3)	325	265	1448	1025	2851	-750	-1500	-800

cyclohexyl substituents preventing the delocalization of lone pair of electrons on nitrogen between  $(R_2)N-C(S_2^-)$  bond. The  $\nu_{C-S}$  bands appear at  $1006\text{ cm}^{-1}$ ,  $1017$  and  $1025\text{ cm}^{-1}$  for (1), (2) and (3) respectively without any splitting, supporting the isobidentate coordination of the dithiocarbamates to the metal centre. In compounds (1), (2) and (3),  $\nu_{C-H}$  vibrations appear in the region of  $2851\text{--}2928\text{ cm}^{-1}$ .

### 3.2.2. Electronic spectral studies

Thallium(III) complexes exhibit fully allowed charge transfer transitions (CT) which appeared as intense absorptions. The characteristic absorption bands were observed around 325 nm for all

**Table 2**  
NMR spectral data (ppm).

Compound	NMR	$\alpha\text{-CH}$	$\beta\text{-CH}_2$	$\gamma\text{-CH}_2$	$\alpha'\text{-CH}_3/$ $CH_2/CH$	$N^{13}CS_2$
(1)	$^1H$	4.64(s)	1.93–1.95(e)	1.65–1.82	3.23	–
	$^{13}C$	66.83	30.05	25.28–25.42	37.16	200.69
(2)	$^1H$	4.62(s)	2.01–2.17(e)	1.60–1.82	3.72	1.30– 1.34(t)
	$^{13}C$	45.51	30.98	21.49–25.65	37.62	13.90
(3)	$^1H$	4.77(s)	1.92–2.21(e)	1.49–1.78	3.37	–
	$^{13}C$	53.74	29.82	–	30.97	–

the three complexes (1), (2) and (3). The intraligand transitions are however observed around 260 nm due to  $\pi-\pi^*$  transitions.

### 3.2.3. Cyclic voltammetric studies

In complex (1), the voltammogram shows the reduction potentials at  $-972$  and  $-1500$  mV. First reduction at  $-972$  mV indicates the first step of the reduction in which  $Tl^{3+}$  complex is reduced to  $Tl^+$ . Second reduction potential at  $-1500$  mV is observed due to the formation of  $Tl^0$  from  $Tl^+$  ion. A similar process is envisaged for (2);  $Tl^{3+}/Tl^+$  redox couple at  $-1117$ , and  $Tl^+/Tl^0$  couple at  $-1566$  mV due to the increase in electron density on ethyl analogue. In the case of (3), a reduction potentials for the same redox couples are observed at  $-750$  and  $-1500$  mV due to steric hindrance in the complex. On the anodic side, all the three complexes showed currents at  $-767$ ,  $-890$  and  $-800$  mV for (1), (2), and (3) respectively due to oxidation of  $Tl^0$  to  $Tl^+$  ion [15]. On the oxidation side, the small currents observed at  $-180$  mV for all three complexes are due to the oxidation of  $Tl^+$  to  $Tl^{3+}$ . The redox processes are highly irreversible.

### 3.2.4. NMR spectral studies

NMR spectral data of the thallium complexes are listed in Table 2.  $^1H$  NMR of complex (1) shows an intense signal at 4.64(s) ppm corresponding to a single proton integration due to  $\alpha\text{-CH}$  of the cyclohexyl ring.  $CH_3$  protons ( $\alpha\text{-CH}_3$ ) attached to the nitrogen appear at 3.23(s) ppm with proton integration corresponding to three. The  $\alpha\text{-CH}$  and  $\alpha'\text{-CH}_3$  protons are affected to a maximum effect by complexation. In the cyclohexyl ring all the equatorial protons are deshielded to a large extent compared with the axial protons. The equatorial protons attached to  $\beta$  and  $\gamma$  carbons appear in the region of 1.93–1.95 ppm [(d),  $J = 7.2$  Hz]. The  $\delta$  equatorial proton appears at 1.80–1.82 ppm [(d),  $J = 8$  Hz]] and the corresponding axial proton at 1.65–1.68 ppm (d,  $J = 12.4$  Hz)

**Table 3**  
Crystal data, data collection and refinement parameters for (1), (2) and (3).

Complex	(1)	(2)	(3)
Empirical formula	C <sub>24</sub> H <sub>42</sub> N <sub>3</sub> S <sub>6</sub> Tl	C <sub>30.50</sub> H <sub>52</sub> N <sub>3</sub> S <sub>6</sub> Tl	C <sub>42.50</sub> H <sub>70</sub> N <sub>3</sub> S <sub>6</sub> Tl
Formula weight	769.34	857.48	1019.75
Crystal dimensions (mm)	0.25 × 0.22 × 0.20	0.30 × 0.25 × 0.17	0.25 × 0.15 × 0.15
Crystal system	trigonal	monoclinic	triclinic
Colour	yellow	yellow	orange
Space group	R $\bar{3}$	P2 <sub>1</sub> /n	P $\bar{1}$
a (Å)	25.819(7)	9.8139(6)	9.6143(4)
b (Å)	25.819(7)	20.9859(12)	15.7787(6)
c (Å)	32.543(7)	18.7125(11)	16.1324(7)
$\alpha$ (°)	90	90	91.612(2)
$\beta$ (°)	90	96.9372(9)	102.553(2)
$\gamma$ (°)	120	90	99.784(2)
U (Å <sup>3</sup> )	18787(8)	3825.7(4)	2348.67(17)
Z	24	4	2
D <sub>calc</sub> (g cm <sup>-3</sup> )	1.632	1.489	1.442
$\mu$ (cm <sup>-1</sup> )	5.576	4.573	3.737
F(000)	9216	1732	1046
$\theta$ (°)	1.10–25.00	5.62–22.85	2.29–25.00
Diffractometer	Bruker APEX-II CCD	Bruker APEX-II CCD	Bruker APEX-II CCD
Scan type	$\omega$ scans	$\omega$ scans	$\omega$ scans
Index ranges	$-30 \leq h \leq 30, -30 \leq k \leq 30, -38 \leq l \leq 38$	$-11 \leq h \leq 11, -25 \leq k \leq 25, -22 \leq l \leq 22$	$-11 \leq h \leq 11, -18 \leq k \leq 18, -19 \leq l \leq 19$
Reflections collected	113546	42102	40534
Unique reflections	7357	6935	8213
Observed reflections	5998	5332	7082
$F_o > 4\sigma(F_o)$			
Weighting scheme	$w = 1/[\sigma^2(F_o^2) + (0.0224P)^2 + 46.1051P]$ , where $P = (F_o^2 + 2F_c^2)/3$	$w = 1/[\sigma^2(F_o^2) + (0.0365P)^2 + 2.8992P]$ , where $P = (F_o^2 + 2F_c^2)/3$	$w = 1/[\sigma^2(F_o^2) + (0.0224P)^2 + 1.2505P]$ , where $P = (F_o^2 + 2F_c^2)/3$
Number of parameters refined	410	388	487
Final R, R <sub>w</sub> (observed data)	0.0484, 0.0296	0.0473, 0.0319	0.0351, 0.0249
Goodness of fit (GOF)	1.066	1.024	1.046

**Table 4**  
Selected bond distances (Å) and bond angles (°) for (1), (2) and (3).

	(1)	(2)	(3)
<i>Bond distances</i>			
Tl(2)–S(3)	2.6075(18)	Tl(1)–S(1)	2.6587(14)
Tl(2)–S(4)	2.6764(18)	Tl(1)–S(2)	2.6529(11)
Tl(2)–S(5)	2.5995(18)	Tl(1)–S(3)	2.6375(14)
Tl(2)–S(6)	2.7230(18)	Tl(1)–S(4)	2.6768(13)
Tl(2)–S(7)	2.6408(19)	Tl(1)–S(5)	2.6805(14)
Tl(2)–S(8)	2.6818(18)	Tl(1)–S(6)	2.6352(14)
C(9)–N(2)	1.312(7)	C(1)–N(1)	1.330(6)
C(17)–N(3)	1.326(7)	C(10)–N(2)	1.323(6)
C(25)–N(4)	1.320(7)	C(19)–N(3)	1.329(6)
<i>Bond angles</i>			
S(3)–Tl(2)–S(4)	68.24(5)	S(1)–Tl(1)–S(2)	68.03(4)
S(5)–Tl(2)–S(6)	67.50(5)	S(3)–Tl(1)–S(4)	67.86(4)
S(7)–Tl(2)–S(8)	67.68(5)	S(5)–Tl(1)–S(6)	67.81(4)
S(3)–C(9)–S(4)	118.6(3)	S(1)–C(1)–S(2)	119.0(3)
S(5)–C(17)–S(6)	119.1(4)	S(3)–C(10)–S(4)	118.4(3)
S(7)–C(25)–S(8)	119.1(4)	S(5)–C(19)–S(6)	118.7(3)
Tl(1)–S(1)	2.5834(10)	Tl(1)–S(2)	2.7697(10)
Tl(1)–S(3)	2.6132(10)	Tl(1)–S(4)	2.6927(10)
Tl(1)–S(5)	2.5451(10)	Tl(1)–S(6)	2.8228(10)
C(1)–N(1)	1.337(4)	C(14)–N(2)	1.327(4)
C(14)–N(2)	1.327(4)	C(27)–N(3)	1.336(4)
S(1)–Tl(1)–S(2)	66.38(3)	S(3)–Tl(1)–S(4)	67.07(3)
S(3)–Tl(1)–S(4)	67.07(3)	S(5)–Tl(1)–S(6)	66.07(3)
S(5)–Tl(1)–S(6)	66.07(3)	S(1)–C(1)–S(2)	117.76(19)
S(1)–C(1)–S(2)	117.76(19)	S(3)–C(14)–S(4)	116.88(19)
S(3)–C(14)–S(4)	116.88(19)	S(5)–C(27)–S(6)	117.4(2)
S(5)–C(27)–S(6)	117.4(2)		

[15]. <sup>13</sup>C NMR spectrum of (1) shows a weak signal at 200.69 ppm due to the characteristic thioureide carbon [15]. The  $\alpha$ -carbon (cyclohexyl ring) appears at 66.83 ppm and  $\alpha'$ -C(H<sub>3</sub>) appears at 37.16 ppm. The  $\gamma$ - and  $\delta$ -carbons are highly shielded and appeared at 25.42 ppm and 25.28 ppm respectively. The  $\beta$ -carbon was deshielded and appeared at 30.05 ppm.

In the case of (2), <sup>1</sup>H NMR of  $\alpha$ -CH proton of the cyclohexyl ring appeared at 4.62(s) ppm and  $\alpha'$ -CH<sub>2</sub> protons at 3.72(m) ppm corresponding to two protons.  $\beta'$ -CH<sub>3</sub> protons of the ethyl group appeared as a well resolved triplet at 1.30–1.34(t) ppm. Apart from these signals, a weak signal observed at 7.18 ppm was due to the aromatic protons of toluene moiety. An intense signal observed at 2.17(s) ppm is due to the methyl protons of toluene which is

present as solvent of crystallization. The proton signals in (2) appeared without much change as observed in (1), slightly deshielded in complex (2) at  $\beta$ ,  $\gamma$ , and  $\delta$  protons in the cyclohexyl ring. <sup>13</sup>C NMR of (2) showed the characteristic thioureide signal at 207.08 ppm.  $\beta'$ (H<sub>3</sub>)C appeared at 13.90 ppm as a much shielded signal and the  $\alpha'$ -CH<sub>2</sub> appeared highly deshielded at 37.62 ppm. <sup>13</sup>C chemical shifts of the cyclic ring appeared similar in both (1) and (2) except for the aromatic signal due to toluene which appeared in the region: 125.32–129.06 ppm.

In complex (3),  $\alpha$ -CH proton of the cyclohexyl ring was observed at 4.77(s) ppm.  $\alpha'$ -CH proton appears at 3.38(s) ppm.  $\beta$ ,  $\beta'$ -CH<sub>2</sub>,  $\gamma$ ,  $\gamma'$ -CH<sub>2</sub> and  $\delta$ ,  $\delta'$ -CH<sub>2</sub> signals appeared in the region of 1.49–1.93(m) ppm. The axial proton signals are observed at

1.24–1.26(m) ppm and a small intense peak observed at 2.35 ppm is due to solvent of crystallization.  $^1\text{H}$  NMR signals of (1), (2) and (3) were found to be quite similar.  $^{13}\text{C}$  NMR spectra exhibited a weak characteristic signal due to thioureide carbon at 207.07 ppm.  $\alpha\text{-C(H)}$  was found to be slightly shielded and appeared at 53.74 ppm.  $\beta\text{-C(H}_2\text{)}$ ,  $\gamma\text{-(CH}_2\text{)}$  and  $\delta\text{-(CH}_2\text{)}$  signals appeared in the region of 24.88–29.37 ppm. In the three complexes, thioureide signals appeared at 200.69 (1), 207.08 (2) 207.07(3) ppm, the least  $^{13}\text{C}$  chemical shift observed for (1) is due to the effective electron releasing methyl group in (1) [21]. Spectra of the complexes clearly indicated that the immediate environment around thioureide nitrogen was largely influenced by complexation.

### 3.2.5. Structural analysis

Details of data collection and refinement parameters for complexes (1), (2), and (3) are given in Table 3. Selected bond distances and angles are given in Table 4. ORTEP of (1) is given in Fig. 4. The compound is monomeric and discrete in nature. Mean Tl–S bond distance of the compound is 2.6548(18) Å. Tl–S bonds and the associated C–S bonds show asymmetry as a requirement of packing. Mean S–Tl–S, and S–C–S angles are 67.81 and 118.9° respectively in (1). The thioureide bond shows a mean value of 1.319(7) Å and indicates a partial double bonded nature of the C–N bond.

ORTEP of (2) is shown in Fig. 5. The complex is monomeric. Tl–S bond lengths (2.6352(14) and 2.6805(14) Å) are noticeably different indicating the asymmetry due to packing requirements. The C–S bonds also show asymmetry as a result of the prevailing asymmetry in Tl–S bonds. Short thioureide bond distances, mean value equivalent to 1.327 Å shows that the electron density is localized over  $\text{S}_2\text{CN}$  moiety and it is partially double bonded in nature. Mean S–Tl–S and S–C–S angles observed in the compound are 67.80° and 118.9° respectively. ORTEP diagram of (3) is shown in Fig. 6. The molecule is monomeric with three short Tl–S bond (mean 2.580 Å) distances occupying triangular face in the coordination polyhedron and other three Tl–S (mean 2.761 Å) distance. Mean of all the six Tl–S bond distances observed in the compound is 2.6711(10) Å. S–Tl–S angles average to 66.51° and the S–C–S angles average to 117.6°.

In general, the complexes show distorted octahedral geometry. With reference to the Tl–S distances, the complexes show an

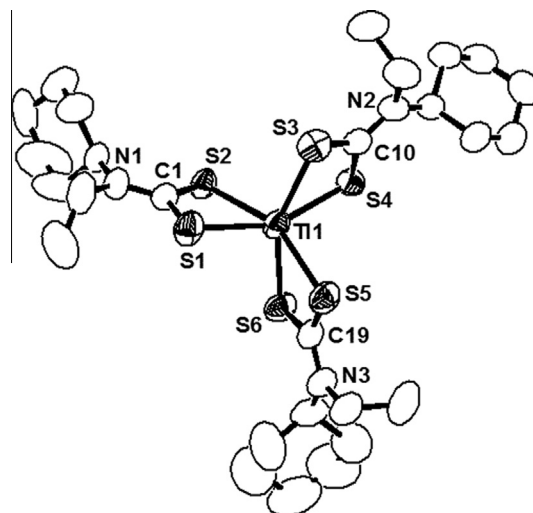


Fig. 5. ORTEP of (2), (hydrogen atoms and solvent of crystallization are excluded for clarity).

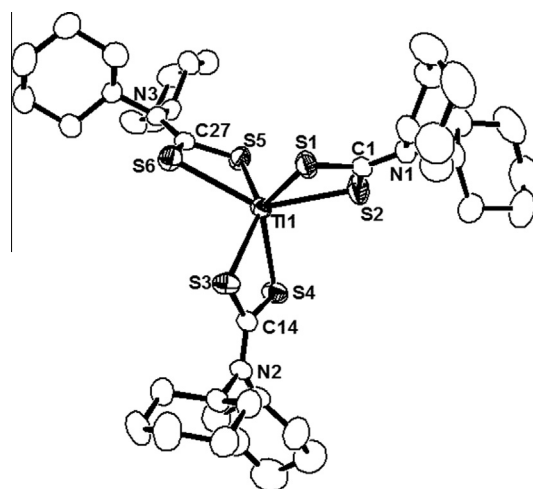


Fig. 6. ORTEP of (3) (hydrogen atoms and solvent of crystallization are excluded for clarity).

increasing trend as follows: (3) > (2) > (1). Mean of the S–Tl–S and S–C–S bond angles are the smallest for (3) among the three compounds. The observations are as a consequence of the steric influence due to two bulky cyclohexyl rings present in (3). Mean thioureide distances are 1.319(7), 1.327(6) and 1.333(4) Å in (1), (2) and (3) respectively. Relatively large thioureide bond distance observed in (3) indicates that the delocalization of the lone pair of electrons on nitrogens is the least in the compound compared to other two. Thallium(I) complexes reported from our laboratory were polymeric in nature [15] whereas all the thallium(III) complexes reported in this paper are discrete and monomeric in nature indicating the hard nature of thallium(III).

## 4. Conclusions

In the present investigation, the ease of formation of thallium sulfide was found to be very high for (3) compared to the other two compounds. Before the solvent started to boil, compound (3) yielded the thallium sulfide compared to the other two compounds. The observation is in line with the longest mean Tl–S and thioureide C–N bonds observed for (3). A strong correlation

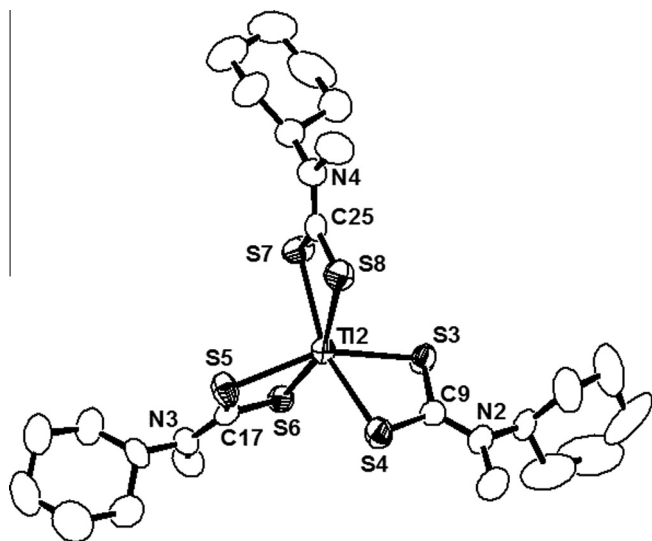


Fig. 4. ORTEP of (1), (hydrogen atoms are excluded for clarity).

exists between the bond strengths of Tl–S, the thioureide C–N and the ease of formation of thallium sulfide, longer the bond distance easier is the formation of the metal sulfide. The *nano* metal sulfide formed is spherical in nature and has been characterized by PXRD, EDX, HRTEM. The precursor dithiocarbamtes show thioureide bands characteristic of their partial double bonded nature. NMR ( $^{13}\text{C}$ ) shows characteristic thioureide carbon in the range: 200.6–207.1 ppm. Single crystal X-ray structural characterization shows that Tl–S and C–S bonds are in general asymmetric in nature. Thioureide bonds of compound (**3**) are the longest. S–Tl–S and S–C–S bond angles of (**3**) are relatively the least in magnitude due to the steric influence.

## References

- [1] J. Goldschmidt, T. Wanger, A. Engelhorn, H. Friedrich, M. Happel, A. Ilango, M. Engelmann, I.W. Stuermer, F.W. Ohl, H. Scheich, *NeuroImage* 49 (1) (2010) 303.
- [2] J. Goldschmidt, W. Zuschratter, H. Scheich, *NeuroImage* 23 (2) (2004) 638.
- [3] S.C. Speller, *Mater. Sci. Technol.* 19 (3) (2003) 269.
- [4] G. William, A. Harter, M. Hermann, Z.Z. Sheng, *Appl. Phys. Lett.* 53 (12) (1988) 1119.
- [5] E.S. Ferreira, M. Mulato, *Braz. J. Phys.* 42 (2012) 186.
- [6] V. Estrella, M.T.S. Nair, P.K. Nair, *Thin Solid Films* 414 (2) (2002) 281.
- [7] A.P. Aliev, Sh.G. Gasimov, T.G. Mamedov, T.S. Mamedov, A.I. Nadjafov, Yu. MirHasan, A.I. Seyidov, *Phys. Solid State* 48 (12) (2006) 2322.
- [8] V. Janickis, R. Stokienė, *Chemija* 21 (1) (2010) 17.
- [9] I.M. Ashraf, H.E. Ishaikh, A.M. Badr, *Cryst. Res. Technol.* 39 (1) (2004) 63.
- [10] A.V. Ivanov, O.A. Bredynk, A.V. Gerasimenko, O.N. Antzutkin, W. Forsling, *Russ. J. Coord. Chem.* 32 (2006) 339.
- [11] G. Marimuthu, K. Ramalingam, C. Rizzoli, M. Arivanandhan, *J. Nanopart. Res.* 14 (2012) 710.
- [12] K. Ramalingam, S. Uma, C. Rizzoli, G. Marimuthu, *J. Coord. Chem.* 63 (2010) 4123.
- [13] G. Marimuthu, K. Ramalingam, C. Rizzoli, *Polyhedron* 29 (2010) 1555.
- [14] C. Rizzoli, K. Ramalingam, N. Alexander, *Acta Crystallogr., Sect. E* 64 (2008) 1020.
- [15] N. Alexander, K. Ramalingam, C. Rizzoli, *Inorg. Chim. Acta* 365 (2011) 480.
- [16] A.C.T. North, D.C. Phillips, F.S. Mathews, *Acta Crystallogr., Sect. A* 24 (1968) 348.
- [17] Bruker, *SADABS* (Version 2007/4), Bruker AXS Inc., Madison, Wisconsin, USA, 2008.
- [18] A. Altomare, M.C. Burla, M. Camalli, G.L. Cascarano, C. Giacovazzo, A. Guagliardi, A.G.G. Moliterni, G. Polidori, R. Spagna, *J. Appl. Crystallogr.* 32 (1999) 115.
- [19] G.M. Sheldrick, *SHELXL 97*, Program for Crystal Structure Refinement, Univ. of Göttingen, Germany, 1997.
- [20] L.J. Farrugia, *ORTEP-3 for Windows*, University of Glasgow, Scotland, UK, 1999.
- [21] H.L.M. Van Gaal, J.W. Diesveld, F.W. Pijpers, J.G.M. Van Der Lindon, *Inorg. Chem.* 18 (1979) 3251.